

See discussions, stats, and author profiles for this publication at: <https://www.researchgate.net/publication/333742446>

Woven Fabric Density Measurement by Using Multi-Scale Convolutional Neural Networks

Article in IEEE Access · June 2019

DOI: 10.1109/ACCESS.2019.2922502

CITATIONS

17

READS

451

6 authors, including:



Shuo Meng

Jiangnan University

9 PUBLICATIONS 177 CITATIONS

SEE PROFILE



Jingan Wang

Jiangnan University

37 PUBLICATIONS 304 CITATIONS

SEE PROFILE



Wentao He

Jiangnan University

12 PUBLICATIONS 89 CITATIONS

SEE PROFILE

Date of publication xxxx 00, 0000, date of current version xxxx 00, 0000.

Digital Object Identifier 10.1109/ACCESS.2017.Doi Number

Woven Fabric Density Measurement by Using Multi-scale Convolutional Neural Networks

Shuo Meng¹, Ruru Pan¹, Weidong Gao¹, Jian Zhou¹, Jingan Wang¹, Wentao He¹

¹Key Laboratory of Eco-textiles, Ministry of Education, Jiangnan University, Wuxi, Jiangsu 214122, China

Corresponding author: Ruru Pan (e-mail: prrs@163.com)

This research was supported in part by the National Key R&D Program of China under Grant 2017YFB0309200, the Fundamental Research Funds for the Central Universities under Grant JUSRP51907A.

ABSTRACT Fabric density measurement plays a key role in the analysis of fabric structural parameters. Existing automatic measurement methods lack varieties adaptability and present poor performance in practical application. In order to solve these problems, we use convolutional neural networks (CNNs) to locate warps and wefts for woven fabric density measurement. First, we use a portable wireless device to capture high resolution fabric images and set up a new dataset with labeled yarns location. Based on this dataset, we propose an effective multi-scale convolutional neural network (MSnet) architecture to locate warps and wefts. Then, by using Hough transform and image projection of predicted yarns location, the fabric density is measured accurately. The experimental results emphasize that the proposed method has reached high accuracy under various kinds of patterns and densities fabrics, and is superior to the state-of-the-art methods in terms of its accuracy and robustness. Promisingly, the proposed method can provide novel ideas for more other fabric structural parameters analysis.

INDEX TERMS Warps and wefts locating, density measurement, fabric structural parameters, multi-scale convolutional neural networks.

I. INTRODUCTION

Material parameters measurement and analysis technology plays an important role in manufacturing industry. In textile industry, fabric structural parameters are first analyzed before mass production. The production of woven fabrics is a major sector within the textile industry. They are produced by interlacing vertically passing warps and horizontally passing wefts according to a predefined weaving pattern and the intersection points between wefts and warps are called float-points [1]. A typical yarn-dyed plain fabric is shown in Fig. 1. Fabric density, which is defined as the number of warps or wefts in a unit length [2], is regarded as one of the most important structural parameters and quality control elements in woven fabrics. Conventional fabric density measurement methods are mainly based on manual measurement, which have high labor costs and low efficiency. Therefore, it is essential to find a convenient and high robustness automatic method for fabric density measurement.

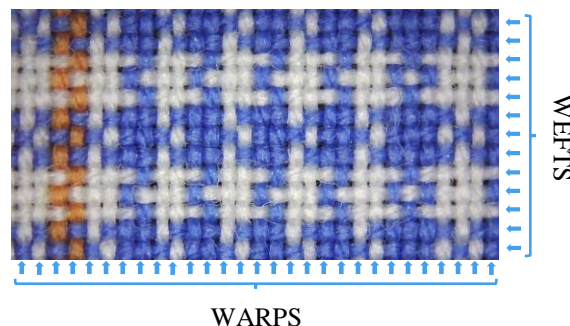


FIGURE 1. A woven fabric image sample.

For automatic fabric density measurement, it is necessary to get the distance between two adjacent yarns. Fig. 2 shows a variety of woven fabric images. It can be observed that: 1) yarn colors, yarn diameters and fabric patterns are diverse; 2) yarns are slant in some fabrics; 3) warps and wefts are masked by each other. These seem to be a rather challenging task, since a method should have high generalization, which does not need to tune parameters for different kinds of fabrics.

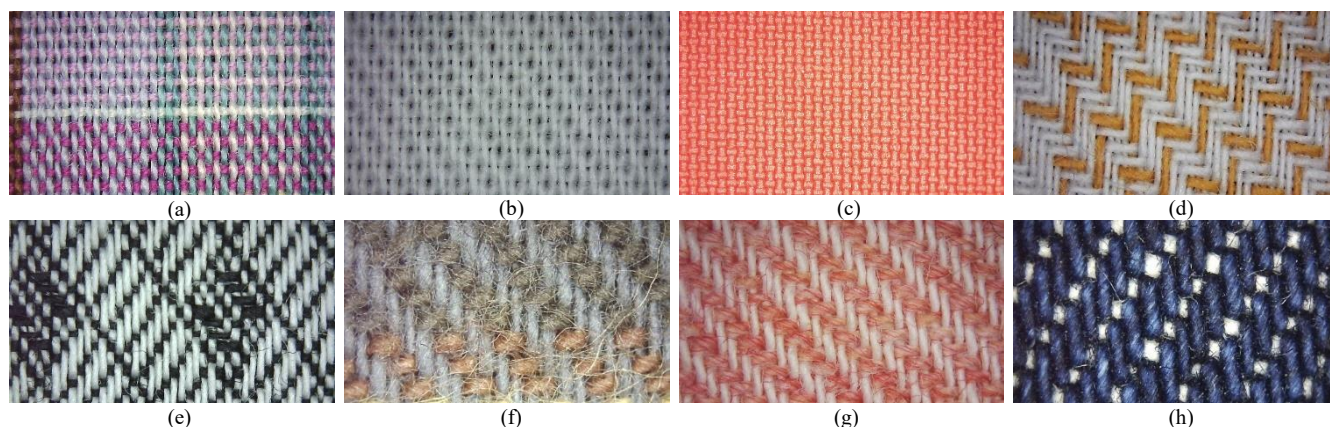


FIGURE 2. Some typical fabric image examples. (a) Yarn-dyed fabric, (b) Solid color fabric, (c) High-tightness fabric, (d) Fabric with skew yarns, (e) Fabric with complex pattern, (f) Slight nap fabric, (g) Fabric with fancy yarns, (h) Denim fabric.

Since the 1990s, scholars have presented many automatic measurement methods and achieved some progress [3-5]. In general, the main workflow of automatic fabric density measurement is fabric image acquisition and image processing.

The fabric images are mainly acquired through industrial cameras [6] or scanners [7, 8]. Due to the influence of fabric pattern and acquisition environment, the accuracy and application of these methods are limited. Therefore, some new acquisition systems have been designed. Zhang *et al.* [9] used two top and bottom placed LED lights to get both reflective and transmission fabric images, which has clearer yarn gaps and is easy for segmentation. This method shows high performance in yarn-dyed fabrics but is not suitable for high-tightness woven fabrics. Zhang *et al.* [10] utilized two high-resolution cameras to capture dual-side reflected images, which acquired more information and improved the accuracy for fabric density measurement. Schneider *et al.* [1] and Kim *et al.* [11] developed an on-loom fabric image acquisition system and measured fabric density in real-time. The above fabric image acquisition systems are expensive and inconvenient. In actual production, producer need to quickly and accurately analyze fabric structural parameters. However, the measurement environment is undetermined and is not always in a laboratory, which limits the industrial application. So, the portability and the application range of the acquisition equipment is highly required.

According to the fabric image processing method, the existing methods can be divided into two types: frequency domain analysis and spatial domain analysis.

The typical frequency domain analysis is Fast Fourier transform (FFT) [4, 8, 12]. The main principle of FFT is to find the peaks in the power spectrum caused by the periodic alignment of warps and wefts. However, the peaks donated the fabric density in power spectrum are often interfered by the weaving pattern and color pattern. Discrete Wavelet transform (DWT) is another widely used frequency domain method to extract warps and wefts

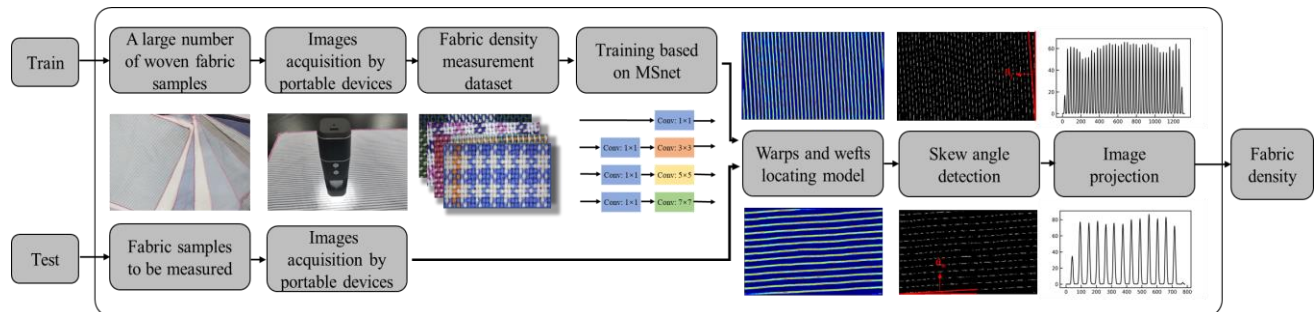
density information [13, 14]. DWT-based methods decompose a fabric image into low and high frequency and reconstruct the horizontal component and vertical component to obtain the warps information and wefts information respectively. The reconstructed images can reflect yarns alignment but yarns are not clearly segmented, which limits its performance. The frequency-domain methods can measure the densities of the solid color fabrics with great accuracy, but the yarn-dyed fabrics with some misjudgments.

Methods based on the spatial domain analysis mainly used co-occurrence matrix [15], quadratic local extremum [16], Hough transform [17]. The above methods measured fabric densities by locating warps and wefts in spatial domain. The ideal yarns locating image is usually an image of warps and wefts with clearly segmented. By utilizing gray-line profile [8] or image projection [17], the warps and wefts density are finally calculated. Similarly, these methods are effective for the analysis of solid color fabrics. Although some methods can deal with yarn-dyed fabrics [18], complex pattern fabrics [6], and high-tightness woven fabrics (HTWF) [19], they all focus on a specific type of fabric. The parameters of their methods need to be adjusted according to different fabric types which has limitations in generalization and varieties adaptability.

Recently, methods based on convolutional neural networks (CNNs) have been made great progress in image processing field such as image segmentation [20], object classification [21, 22]. For automatic fabric density measurement, it is essential to locating and warps and wefts. So far, there have been many effective CNN-based methods for objects locating to solve various problems such as crowd density estimation [23, 24], fish or cell locating [25, 26], facial landmark detection [27, 28]. Unlike their problems, yarns in fabric images are strip-shaped and it is necessary to get the distance between two adjacent yarns. In textile industry, the CNN-based methods are mainly used to address fabric defect detection [29] and fabric images retrieval [30]. There are still few studies about fabric density measurement based on CNNs as far as we know.

TABLE 1. Some typical methods in recent years and their performance.

| Article | Image acquisition system | Method | Fabric types | Error | Processing time |
|----------------------|--------------------------|----------------------------------|------------------------|-----------------|-----------------|
| Pan et al. [19] | Backlighting system | FFT | solid color & HTWF | 1.22% | 15s |
| Zhang et al. [7] | Scanner | Sub-images projection | complex pattern fabric | 0.09% | 1.9 s |
| Aldemir et al. [6] | Camera | Gabor filter & gray line profile | yarn-dyed fabric | 5% | NAN |
| Schneider et al. [1] | On-loom system | Tracking single yarn | solid color fabric | ± 1 yarn/cm | ≤ 28 s |
| Zhang et al. [10] | Dual-side camera | Dual-side image & FFT | yarn-dyed fabric | 0.56% | 1.86s |
| Jing et al. [13] | Scanner | Wavelet Transform | yarn-dyed fabric | 0.08% | NAN |
| Wang et al. [16] | Scanner | Quadratic local extremum | solid color fabric | 0 | 3s |

**FIGURE 3. Flow chart of the proposed method.**

In summary, Table 1 shows some typical fabric density measurement methods in recent years and their performance. Although many automatic methods based on image processing have been reached high accuracy and efficiency, they are usually suitable for a certain fabric type and the image acquisition equipment is inconvenient and expensive. All the above drawbacks limit the further industrial application. In this paper, we aim to conduct accurate fabric density measurement for all kinds of woven fabrics with uniform density. Inspired by the strong feature learning capability of CNNs, we use an effective multi-scale convolutional neural network (MSnet) to locate yarns for automatic fabric density measurement. The flow chart of the proposed method is shown in Fig. 3. It can accurately and effectively locate yarns in clear woven fabric images, which overcomes the deficiency of the traditional fabric density measurement methods.

The rest of paper is organized as follows. In Section II, we first briefly introduce the image acquisition system and the dataset establishment. Then, in Section III, we provide a description of the proposed method which includes the MSnet for yarns locating and fabric density measurement based on the predicted location maps. Section IV describes the implement details and the results of the experiments. In Section V, we discuss some parameter settings and make comparisons with different automatic measurement methods. Final Section VI concludes this paper.

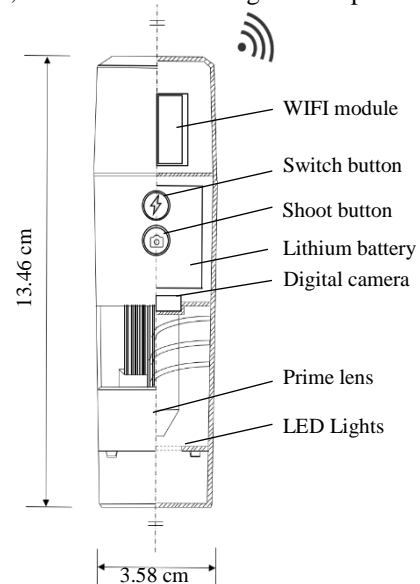
II. IMAGE ACQUISITION SYSTEM AND DATASET ESTABLISHMENT

A. IMAGE ACQUISITION SYSTEM

A new portable wireless device is used to capture high-resolution fabric images in sRGB mode, which is shown in Fig. 4. The core of the device is a digital camera equipped

with a prime lens and an WIFI module. The distance between the lens and the fabric is fixed so as to acquire clear images. Below the lens, it has 8 small LED lights to provide illumination. When the shoot button is pressed, the captured image is transferred wirelessly by the interior WIFI module to a sever. Because the device uses the wireless connection and the small size, the application range and the portability are greatly increased.

During the image acquisition, the device should be placed closely to the surface of a flat fabric sample. Only in this way can get a clear image and the spatial resolution (PPI) can be fixed. The resolution is set as 4680 pixel/inch and the image size is 1280 pixels \times 720 pixels. On the other hand, it is no need to distinguish warps and wefts.

**FIGURE 4. A portable fabric image acquisition device.**

B. DATASET ESTABLISHMENT

We collected about 400 kinds of fabrics with detailed parameters and used the above image acquisition system to capture their high-resolution images. It should be noted that as long as fabric images with clear yarns and certain resolution are obtained, the fabric densities can be measured. The proposed method does not rely on the image acquisition system. Fig. 2 shows some representative samples of this dataset.

To measure the fabric density in a given image via the CNNs, there are two options. One is a network whose input is the image and the output is the estimated fabric density. The other is to output the location of each yarn and then calculate the density. In this paper, we are in favor of the second choice for the following reasons:

- (1) Yarns location contains more information. Compared to the final estimated fabric density, yarns location gives the spatial distribution of the yarns, which can be used in other fabric parameters analysis such as float-points identification, fabric pattern analysis.
- (2) Directly predicting fabric density shows low performance in our experiments.

For the above reasons, we labeled yarns outline in 600 images of about 400 kinds of fabrics. The model needs to be trained to estimate the yarns location from input fabric images. Moreover, Yarns should be segmented clearly from the predicted yarns location images for subsequent fabric density measurement, so the quality of ground truth given in the dataset influences the performance of our method. Because yarns are touched with each other and their shapes are strip, it is not suitable for changing the

problem into a binary-classification segmentation work or using Gaussian kernel to locate yarns. Therefore, in this work, we introduce a new method to convert an image with labeled yarns outline to warps and wefts location maps, which just like a heatmap. Fig. 5 shows a labeled image and converted wefts location map. First, warps and wefts are processed individually for every labeled image. A three-channel image is converted into a two-channel location map of warps and wefts. Then, for pixel x in labeled yarns outline, we assume it obeys the Gaussian probability distribution with the yarn center μ as the mean and a scale parameter σ as the standard deviation, which is shown as follows.

$$f(x) = \frac{1}{\sqrt{2\pi}\sigma} \exp\left(-\frac{(x-\mu)^2}{2\sigma^2}\right) \quad (1)$$

$$\mu = \frac{d_y}{2}, \quad \sigma = \varphi d_y \quad (2)$$

where $f(x)$ denotes the value of pixel x , d_y is yarn diameter, μ is set as the central position of yarn outline, σ is positively related to yarn diameter, φ is a non-negative weight.

To avoid the value on the yarn boundary become too small in large diameter yarns, we set the value of σ vary with yarn diameter rather than a fixed value. σ is positively related to yarn diameter, which means the larger the value of σ , the flatter the distribution. In this way, the converted location map contains all yarns outline information and in the center of the yarn has the max value. We set φ as 0.01 of the outlines by experiments.

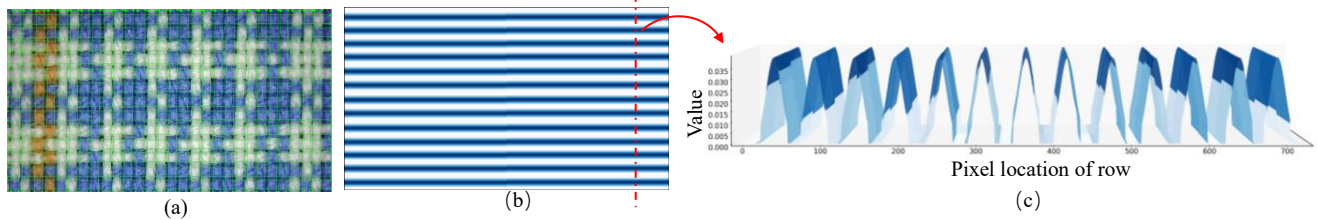


FIGURE 5. Labeled image of Fig. 1 and its location map. (a) Labeled image of Fig. 1, (b) Converted wefts location map, (c) Wefts profile map

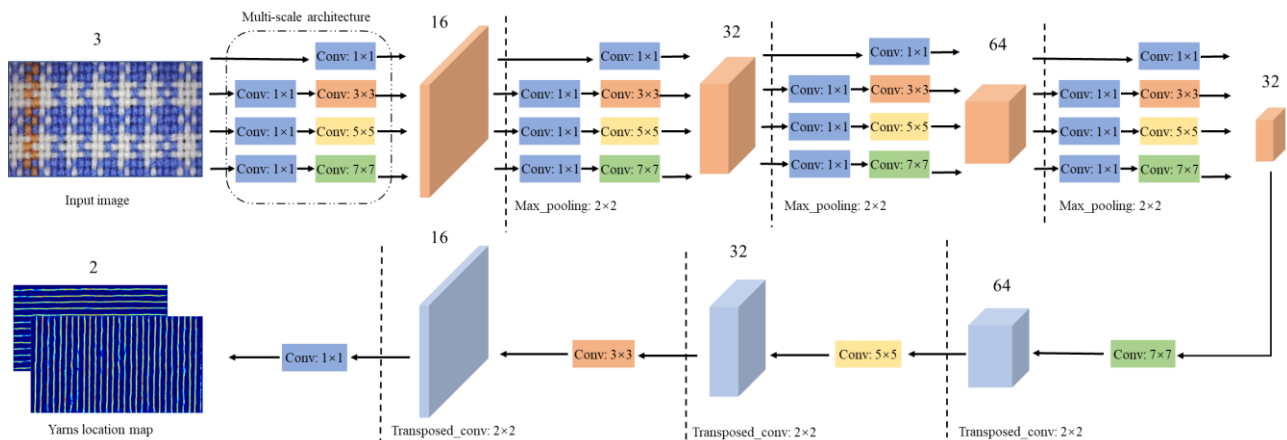


FIGURE 6. The structure of the proposed MSnet for yarns locating.

III. THE PROPOSED METHOD

Current automatic fabric density measurement methods lack adaptability. Their methods rely heavily on the feature extracted method. In this section, we first propose a multi-scale convolutional neural network (MSnet) architecture to locate the warps and wefts in various fabric images. Then, we introduce the fabric density measurement method based on the predicted yarns location maps.

A. MULTI-SCALE CONVOLUTIONAL NEURAL NETWORK

1) ARCHITECTURE

The architecture of the proposed MSnet is illustrated in Fig. 5. It is inspired by the fully convolutional networks, which has been validated in many image processing tasks. The overall idea of our approach is to eliminate most yarns texture noises by retaining only robust location features. Then, by using transposed convolution, we do pixel-wise prediction. The architecture contains two components: multi-scale feature encoder and yarns location map decoder.

(1) Multi-scale feature encoder:

Because yarn diameters and fabric densities are diverse, it is more suitable to use filters with different sizes of local receptive field to learn from the raw image to the location map. Inspired by the success of Inception structure[21], we use a concatenation structure with four multi-scale modules to learn the feature of the raw input image. In this paper, the filter size of each module is 1×1 , 3×3 , 5×5 , 7×7 and a 1×1 filter is added before them to reduce the feature dimensions. The output channel of each module is 16, 32, 64, 32 and each interior branch is equal for simplicity. A 2×2 max-pooling layer is applied after each module except the last one, which helps retaining only robust features.

(2) Yarns location map decoder:

In order to generate high-resolution yarns location map, we use four convolutional layers with filter size of 7×7 , 5×5 , 3×3 , 1×1 to refine the details of feature maps. The output channel of each hidden layer is 64, 32, 16. Three 2×2 transposed convolutional layers are added among them to reconstruct the spatial resolution and do pixel-wise prediction. The final outputs are two location maps of warps and wefts. Their sizes are as same as the input image. Since the values of location maps are always non-negative, we apply ReLU activation in every layer.

2) LOSS FUNCTION

For the purpose of conducting accurate fabric density measurement, it is crucial to get high precision estimated yarns location map. Hence, we combine the mean square error (MSE) with the structural similarity index (SSIM) [31] to measure estimation error and get high-resolution image for subsequent fabric density measurement.

(1) Mean square error:

MSE is computed the error between predicted map and ground truth at each pixel. It is based on the pixel independence hypothesis and ignores the local correlation which only represents the pixel error. MSE can keep overall optimization direction and keep training stable. The loss function is defined as follows:

$$MSE = \frac{1}{N} \sum_{i=1}^N (G_i - Y_i)^2 \quad (3)$$

where N denotes total pixel number of an image, Y_i denotes the predicted value, the G_i denotes the ground truth.

(2) Structural similarity index:

SSIM considers the structural similarity of two images and represents the local correlation, which is closer to human vision system. To avoid overfitting and improve the resolution of the predicted images, we introduce SSIM as regularization to improve the quality of model. SSIM ranges from 0 to 1. When two images are identical, the SSIM value is equal to 1. The loss function is defined as follows:

$$\mu_Y = \frac{1}{N} \sum_{i=1}^N Y_i \quad (4)$$

$$\mu_G = \frac{1}{N} \sum_{i=1}^N G_i \quad (5)$$

$$\sigma_Y^2 = \frac{1}{N-1} \sum_{i=1}^N Y_i - \mu_Y \quad (6)$$

$$\sigma_G^2 = \frac{1}{N-1} \sum_{i=1}^N G_i - \mu_G \quad (7)$$

$$\sigma_{YG} = \frac{1}{N-1} \sum_{i=1}^N (Y_i - \mu_Y)(G_i - \mu_G) \quad (8)$$

$$SSIM = \frac{(2\mu_Y\mu_G + C_1)(2\sigma_{YG} + C_2)}{(\mu_Y^2 + \mu_G^2 + C_1)(\sigma_Y^2 + \sigma_G^2 + C_2)} \quad (9)$$

where μ_Y and σ_Y^2 denote the local mean and variance of the predicted value, μ_G and σ_G^2 denote the local mean and variance of the ground truth, σ_{YG} denotes local covariance, C_1 and C_2 are small constants to avoid division by zero.

The loss function is the combination of MSE and SSIM, which is defined as follows:

$$L = MSE + \lambda(1 - SSIM) \quad (10)$$

where λ is a weight to balance the MSE and SSIM. In this paper, we set λ as 0.001 by experiments.

When a raw fabric image is input, the model will output the warps and wefts location maps. So, we set the final loss function as the sum of the warps and wefts predicted loss. A fabric image sample and its predicted location map is show in Fig. 7 (a-d).

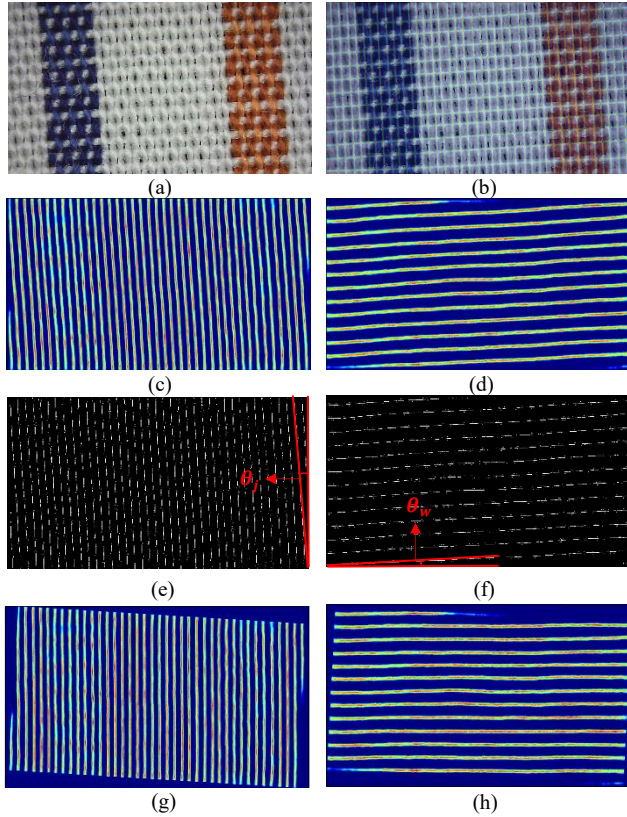


FIGURE 7. Processes of fabric density measurement. (a) Original image, (b) Mixed image of the location maps and the original image, (c) Predicted warps location map, (d) Predicted wefts location map, (e) Skeletonized image of warps location map, (f) Skeletonized image of wefts location map, (g) Rotated warps location map, (h) Rotated wefts location map.

B. FABRIC DENSITY MEASUREMENT BASED ON PREDICTED IMAGES.

1) SKEW ANGLE DETECTION

The slant of yarns in a fabric image cannot be avoided due to the fabric placement as well as warps and wefts are skew in some fabrics. To realize the precise measurement of fabric density, Hough transform [32] is carried out to detect the skew angles of wefts and warps in predicted yarns location maps. To save computation time, we first convert the predicted location map to a binary image by the Otsu algorithm [33]. Then, we use Zhang-Suen thinning algorithm [34] to skeletonize the binary image. Fig. 7 (e) and (f) shows the skeletonized image of the location map. Next, all the pixels in the image from X and Y coordinates (x, y) is converted to polar coordinates (s, θ) as follow:

$$s = x \cdot \cos \theta + y \cdot \sin \theta \quad (11)$$

where θ with the highest frequency is regarded as the skew angle of the yarns. After the above steps, the θ_w and θ_j can be detected. The predicted yarns location maps are rotated $-\theta_w$ and $-\theta_j$ respectively. We use 0 padding for the border of the image. A rotated yarns location map can be seen in Fig. 7 (g) and (h).

2) FABRIC DENSITY MEASUREMENT

After getting the rotated yarns location map, we use grey levels projection to get the distance between two adjacent

yarns. The warps location map is projected in column and the wefts location map is projected in row. The projection curve is smoothed by a minimum filter to remove noise points. The final smoothed projection curve is shown in Fig. 8.

The yarns can be segmented automatically by locating the maxima in Fig 9 (a) and (b). The pixel distance between two adjacent yarns (p) can be obtained by calculating the average value of two adjacent yarns distance in the smoothed projection. The final fabric density can be derived as follow:

$$d_w = \frac{2.54 \times \text{PPI}}{p} \quad (12)$$

$$d_j = \frac{2.54 \times \text{PPI}}{p} \quad (13)$$

where d_w is wefts density (thds/inch), d_j is warps density (thds/inch), PPI is the spatial resolution (pixel/inch), p is the pixel distance between two adjacent yarns (pixel).

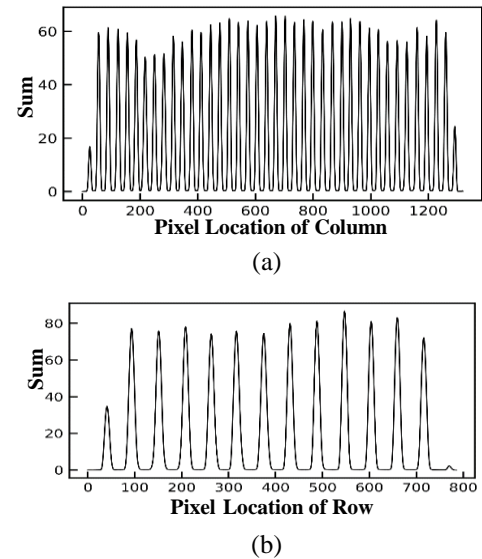


FIGURE 8. Smoothed projection curve of a sample. (a) Warps projection curve, (b) Wefts projection curve.

IV. EXPERIMENTS

To evaluate the effectiveness of our proposed method, we conduct a series of experiments based on the proposed dataset. All the experiments are conducted on a sever with an Intel(R) Core (TM) i9-7900x CPU, GTX 1080Ti GPU and 32 GB RAM memory. The algorithm is implemented on the framework of Keras 2.2.4 with Tensorflow 1.13.0 as backend.

A. DATASET FOR EXPERIMENTS.

The establishment of the dataset has been introduced previously. The dataset contains 600 different images in total for about 400 kinds of fabrics. Some typical samples of this dataset are shown in Fig. 2. Fig. 9 shows the distribution of the warps and wefts densities and fabric types. The dataset covers a wide range of fabric densities and types such as common pattern fabrics, complex pattern

fabrics, yarn-dyed fabrics and high-tightness fabrics. Before model training, the dataset is randomly divided into two parts: 500 images are used for training and the remaining 100 images for testing.

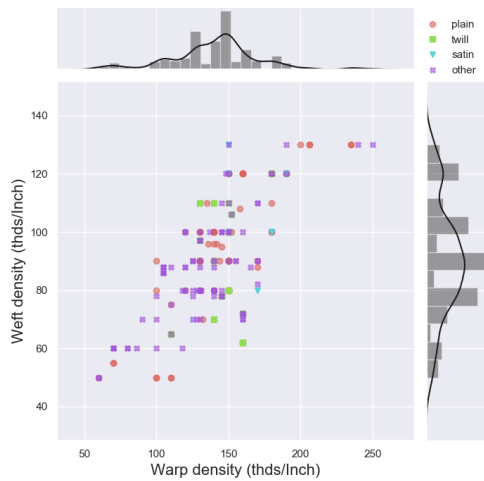


FIGURE 9. The distribution of the warps and wefts densities and fabric types in dataset

B. TRAINING DETAILS.

In model training stage, 5% of the training set is randomly selected as the validation set. In view of the output of the model, the network parameters are randomly initialized by Glorot uniform initializer [35]. Adam optimizer [36] with a small learning rate of 10^{-5} is used to train the model. Data augmentation is essential to training the model to obtain the desired invariance and robustness properties. The images in the original training set and validation set are horizontal flipped, vertical flipped and shifted channel intensity for data augmentation. All these data augmentation methods have no influence on the resolution of images. The final size of training set and validation set is 1900 and 100 images respectively. At the same time, all the images are normalized to $[0, 1]$ for input. After 200 epochs of training, the yarns locating model is obtained.

C. EVALUATION DETAILS.

To evaluate the accuracy of the model prediction, we calculate the root-mean-square error (RMSE) between predicted location maps and the ground truth in testing set. The RMSE is the square root of MSE. Only using RMSE cannot demonstrate the performance of our model for fabric density measurement. So, by following the convention of existing works [6, 12], we calculate the mean-absolute-percentage error (MAPE) between automatic and manual fabric density. The manual fabric density is measured according to [2]. MAPE is defined as follow:

$$MAPE = \frac{1}{N} \sum_{i=1}^N \frac{|G_i - Y_i|}{G_i} \times 100\% \quad (14)$$

where N is the number of test images, G_i is manual measurement value, Y_i is automatic measurement value.

MAPE indicates the accuracy of the estimates. Most of existing works only used MAPE to evaluate the

performances of fabric density measurement. To further evaluate the robustness of the model, we use the mean-squared-percentage error (MSPE), which defined as follows:

$$MSPE = \sqrt{\frac{1}{N} \sum_{i=1}^N \left(\frac{G_i - Y_i}{G_i} \right)^2} \times 100\% \quad (15)$$

MSPE measures the robustness of the estimates, because MSPE is sensitive to outliers and it would be large when the model poorly performs on some samples.

D. RESULTS.

Fig. 10 shows the distribution of warps and wefts density predicted error for each sample in testing set. Fig. 11 and Table 2 show some representative predicted location maps in testing set and their predicted results. The results show that the model successfully locates warps and wefts. The MAPE of warps and wefts density in the testing set is 1.03% and 1.09% respectively, the MSPE is 1.58% and 1.33% respectively. The results indicate that the proposed method shows high accuracy and robustness.

In terms of computation time, it takes about 2.83s for the first loading of the model. But each subsequent computation takes only about 0.48s. At the same time, because of using portable device to capture fabric images, the total consumption time for one measurement is less than 10s. The proposed method shows high efficiency in automatic fabric density measurement.

Due to warps and wefts masked by each other, it shows some deficiency in the binding of warps and wefts in some predicted location maps. On the other hand, the method has a small measurement length due to the high resolution. But all the above effects have a little influence on the accuracy of fabric density measurement. The model shows relative high error when deal with some more complex fabrics such as denim fabrics. The main reasons are that: 1) the sample size of such classes is relatively small, 2) the number of yarns in an image is small, and 3) it is hard to distinguish warps and wefts in images.

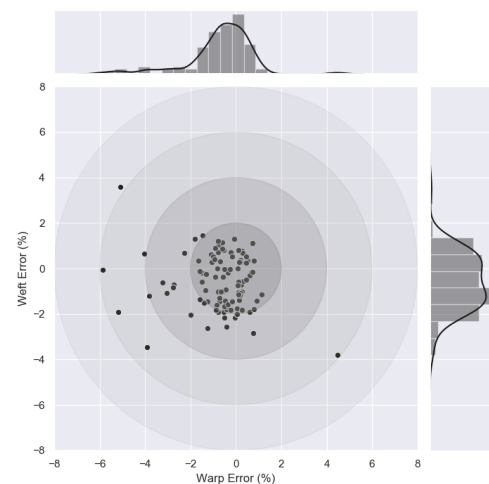


FIGURE 10. The distribution of warps and wefts density MAPE.

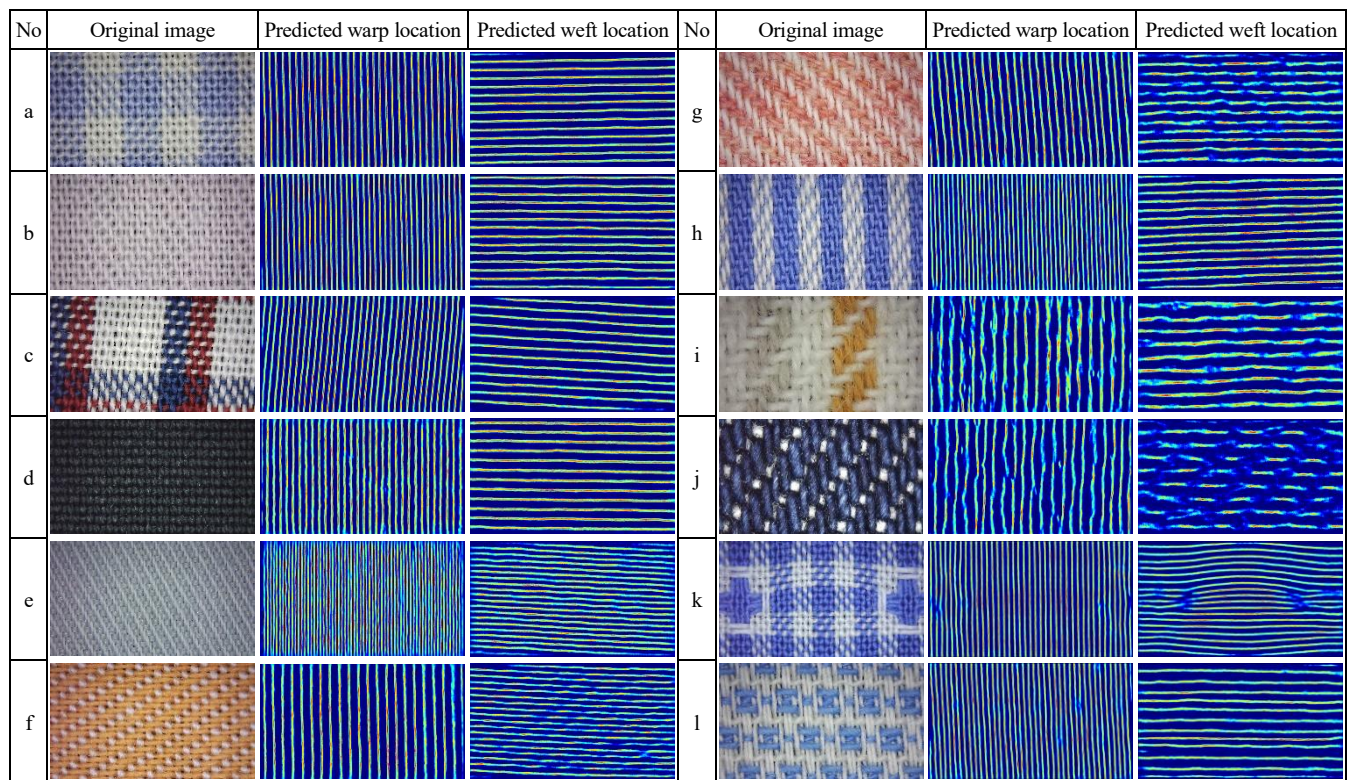


FIGURE 11. Some representative predicted location map in testing set.

TABLE 2. Warp and Weft Densities of Manual and Automatic Measurements.

| Sample No | Fabric types | Manual density (thds/inch) | | Automatic density (thds/inch) | | MAPE (%) | |
|-----------|------------------------|----------------------------|------|-------------------------------|--------|----------|------|
| | | Warp | Weft | Warp | Weft | Warp | Weft |
| a | Yarn-dyed plain fabric | 117 | 89 | 117.07 | 88.66 | 0.06 | 0.38 |
| b | Twill fabric | 140 | 90 | 139.14 | 90.21 | 0.61 | 0.23 |
| c | Slant yarn-dyed fabric | 125 | 80 | 125.1 | 80.1 | 0.08 | 0.12 |
| d | Pure black fabric | 117 | 80 | 117.27 | 78.75 | 0.23 | 1.56 |
| e | High-tightness fabric | 245 | 130 | 243.39 | 130.12 | 0.66 | 0.09 |
| f | Opposite warp and weft | 120 | 80 | 120.29 | 79.43 | 0.24 | 0.71 |
| g | Fancy yarns fabric | 100 | 80 | 98.47 | 78.9 | 1.53 | 1.37 |
| h | Complex pattern fabric | 165 | 90 | 164.73 | 88.38 | 0.16 | 1.80 |
| i | Slight nap fabric | 75 | 60 | 74.65 | 60.37 | 0.47 | 0.62 |
| j | Denim fabric | 75 | 60 | 77.09 | 57.54 | 2.79 | 4.10 |

The proposed method is mainly used to accurately measure fabric density for all kinds of fabrics with uniform density and yarns can be clearly distinguished via an image. Due to some fabrics are composed of curved yarns and some fabrics have nonuniform density, it cannot measure their densities accurately by an image. Even so, our model shows promising results in locating warps and wefts, which is shown in Fig. 11 (k), (l). The results show high potential for other image-based fabric analysis, such as fabric float-point locating, fabric defect detection.

V. DISCUSSION

In this section, we first discuss some parameter settings of the proposed method and some structures used in our MSnet. Then, we make comparisons between the proposed method and other fabric density measurement methods.

A. PARAMETER SETTINGS FOR TRANSFORMING YARN LABELS TO YARNS LOCATION MAPS

The quality of ground truth for training model determines the performance of our method. We separately set fixed σ and adaptive σ (different φ) to evaluate the model performance. Fig. 12 (a-f) shows predicted location maps with different parameters for qualitative analysis. Table 3 reports the testing error with different yarn labeled parameters. Although the model shows great difference in RMSE, both fixed σ and adaptive σ can measure fabric density. When used a proper φ , the adaptive σ has better MAPE and MSPE than fixed σ . This mainly because when using fixed σ , the model shows differences when faced with different yarn diameters. This leads to the instability of the model, which shows high MSPE. Based on the test results, we set $\varphi = 0.1$.

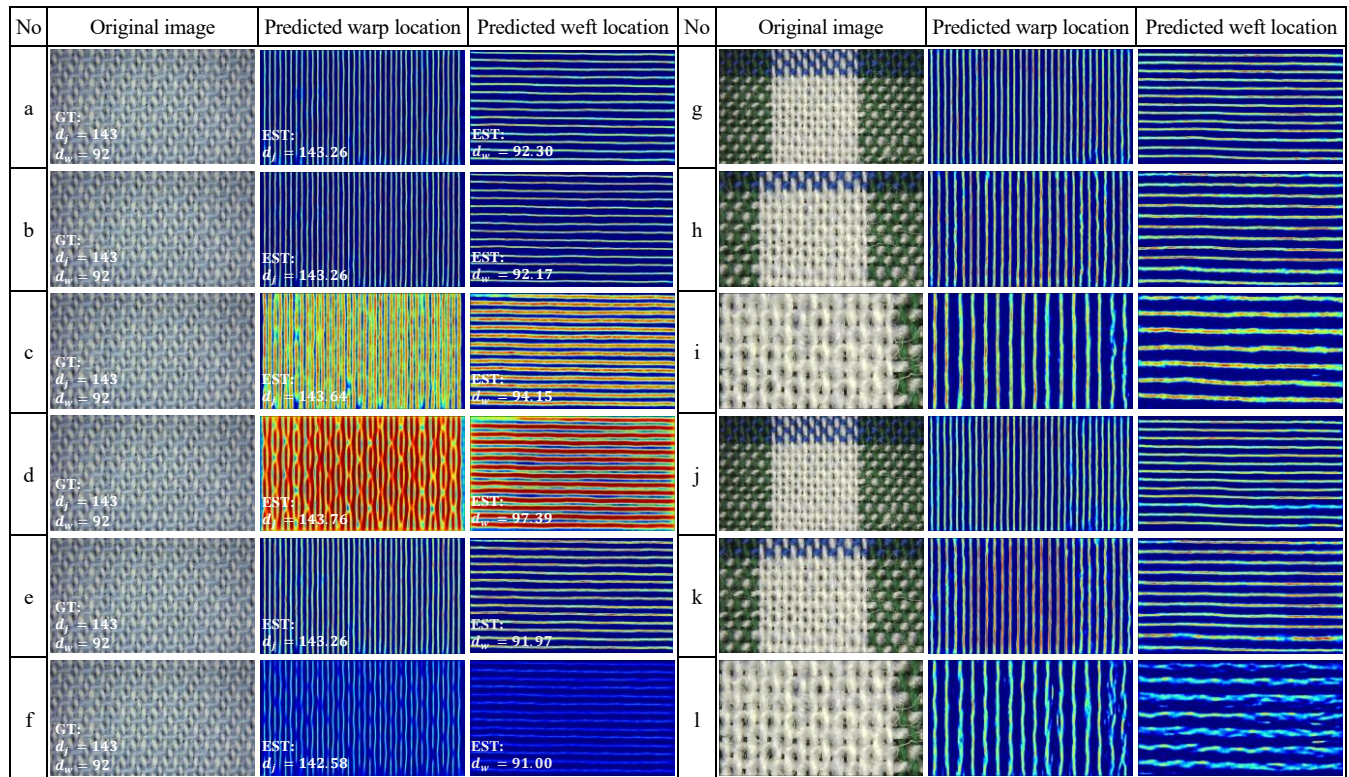


FIGURE 12. Predicted location maps with different parameters and image resolution for qualitative analysis. (a) $\sigma = 0.1$, (b) $\sigma = 1$, (c) $\sigma = 10$, (d) $\varphi = 1$, (e) $\varphi = 0.1$, (f) $\varphi = 0.01$, (g) MSnet with image PPI: 4680, (h) MSnet with image PPI: 5850, (i) MSnet with image PPI: 9360, (j) 3×3 filter net with image PPI: 4680, (k) 3×3 filter net with image PPI: 5850, (l) 3×3 filter net with image PPI: 9360.

TABLE 3. Testing errors of MSnet trained with different yarn labeled parameters.

| Parameter settings | RMSE | MAPE (%) | | MSPE (%) | |
|--------------------|--------------|-------------|-------------|-------------|-------------|
| | | Warp | Weft | Warp | Weft |
| $\sigma = 0.1$ | 0.575 | 1.47 | 1.89 | 4.53 | 4.32 |
| $\sigma = 1$ | 0.068 | 1.14 | 1.41 | 2.00 | 2.38 |
| $\sigma = 10$ | 0.008 | 2.80 | 2.44 | 5.64 | 4.07 |
| $\varphi = 1$ | 0.662 | 2.56 | 2.88 | 6.14 | 6.22 |
| $\varphi = 0.1$ | 0.028 | 1.03 | 1.09 | 1.58 | 1.33 |
| $\varphi = 0.01$ | 0.145 | 1.95 | 1.97 | 4.81 | 5.02 |

B. LOSS FUNCTION DISCUSSION

The results by using the combination of mean square error (MSE) and structural similarity index (SSIM) is given in Table 4. We can observe that training by different loss functions almost have same RMSE. But the model trained with the combined loss results in lower MAPE and MSPE than using only MSE, which indicates that using penalty term of SSIM loss can improve the accuracy and robustness. To find a suitable λ , we use different λ to train the model. As show in Table 4, too large or too small λ will affect the capability of the model. When $\lambda=0.001$, the model shows high performance.

TABLE 4. Testing errors of MSnet trained with different loss functions.

| Parameter settings | RMSE | MAPE (%) | | MSPE (%) | |
|--------------------|--------------|-------------|-------------|-------------|-------------|
| | | Warp | Weft | Warp | Weft |
| $\lambda = 0$ | 0.028 | 2.19 | 1.94 | 5.48 | 5.59 |
| $\lambda = 0.1$ | 0.029 | 1.77 | 1.64 | 3.88 | 4.42 |
| $\lambda = 0.01$ | 0.029 | 1.23 | 1.67 | 2.03 | 3.50 |
| $\lambda = 0.001$ | 0.028 | 1.03 | 1.09 | 1.58 | 1.33 |
| $\lambda = 0.0001$ | 0.028 | 1.54 | 1.41 | 3.45 | 3.03 |

C. INPUT IMAGE RESOLUTION

We evaluated the performance of the proposed method when input different image resolutions with same image size. As illustrated in Table 5, the model can accurately locate the warps and wefts across different resolution. But the higher the resolution, the worse the accuracy of the model. The reason is that a high-resolution image usually contains fewer yarns, which increases the error.

TABLE 5. Comparison with different net structures and image resolutions.

| Model | Image resolution (pixel/inch) | MAPE (%) | | MSPE (%) | |
|---------------------|-------------------------------|-------------|-------------|-------------|-------------|
| | | Warp | Weft | Warp | Weft |
| 3×3 filter | 4680 | 1.35 | 1.64 | 2.65 | 2.90 |
| MSnet | 4680 | 1.03 | 1.09 | 1.58 | 1.33 |
| 3×3 filter | 5850 | 2.53 | 2.65 | 3.75 | 3.58 |
| MSnet | 5850 | 1.58 | 1.67 | 3.39 | 3.51 |
| 3×3 filter | 9360 | 4.56 | 4.45 | 7.23 | 7.08 |
| MSnet | 9360 | 2.15 | 2.36 | 4.05 | 4.68 |

D. MULTI-SCALE STRUCTURE

To evaluate the effectiveness of the multi-scale structure, we separately used the multi-scale structure and used 3×3 filter to take place of all the multi-scale structure. The training parameters of the above two model are nearly equal, which is about 1.6 million. As shown in Table 5, the multi-scale structure obtains more promising results, especially it has lower MSPE. The multi-scale structure is relatively stable when faced with different image resolutions. It is mainly because this structure can take into account a wider context

when making a prediction for a pixel. Fig. 12 (g-l) shows the results with different image resolutions and structures.

TABLE 6. Testing errors and processing times of different methods.

| Method | MAPE (%) | | MSPE (%) | | Processing time (s) |
|-----------------------|-------------|-------------|-------------|-------------|---------------------|
| | Warp | Weft | Warp | Weft | |
| FFT [8, 12] | 11.85 | 12.12 | 23.22 | 17.58 | 2.85 |
| Hough transform [17] | 10.55 | 8.25 | 17.22 | 16.35 | 1.56 |
| Gray line profile [6] | 8.55 | 9.54 | 15.22 | 11.20 | 0.72 |
| Modified VGG [37] | 5.46 | 5.63 | 8.09 | 7.60 | 0.46 |
| Modified MSnet | 5.51 | 7.49 | 8.56 | 12.06 | 0.38 |
| MSnet | 1.03 | 1.09 | 1.58 | 1.33 | 2.88 |

TABLE 7. Modified VGG16 and MSnet configuration.

| ConvNet Configuration | | | |
|----------------------------------|-----------|----------------|----------------|
| Modified VGG16 | | Modified MSnet | |
| Input (720 × 1280 × 3 RGB image) | | | |
| Block 1 | Conv3-64 | Block 1 | Multi-scale 16 |
| | Conv3-64 | | |
| Maxpooling 2 × 2 | | | |
| Dropout 0.1 | | | |
| Block 2 | Conv3-128 | Block 2 | Multi-scale 32 |
| | Conv3-128 | | |
| Maxpooling 2 × 2 | | | |
| Dropout 0.1 | | | |
| Block 3 | Conv3-256 | Block 3 | Multi-scale 64 |
| | Conv3-256 | | |
| | Conv3-256 | | |
| Maxpooling 2 × 2 | | | |
| Dropout 0.1 | | | |
| Block 4 | Conv3-512 | Block 4 | Multi-scale 32 |
| | Conv3-512 | | |
| | Conv3-512 | | |
| Maxpooling 2 × 2 | | | |
| Dropout 0.1 | | | |
| Block 5 | Conv3-512 | Block 5 | Multi-scale 16 |
| | Conv3-512 | | |
| | Conv3-512 | | |
| Maxpooling 2 × 2 | | | |
| Dropout 0.1 | | | |
| Block 6 | Conv3-256 | Block 6 | Multi-scale 8 |
| | Conv3-256 | | |
| | | | |
| Maxpooling 2 × 2 | | | |
| Dropout 0.1 | | | |
| Block 7 | Conv3-128 | FC 2 | |
| | Conv3-128 | ReLU | |
| Maxpooling 2 × 2 | | | |
| Dropout 0.1 | | | |
| Block 8 | Conv3-64 | | |
| | Conv3-64 | | |
| Maxpooling 2 × 2 | | | |
| Dropout 0.1 | | | |
| FC 2 | | | |
| ReLU | | | |

E. COMPARISONS BETWEEN DIFFERENT METHODS

To demonstrate the effectiveness of the proposed method, we carried out some experiments by using different existing automatic fabric density measurement methods. Their methods failed to adapt to all fabric samples in the testing set, and many outliers occur. We ignored some outliers and compared with the proposed method. As given in Table 6, the comparison results show that the proposed method achieves

superior MAPE and MSPE, which verifies the accuracy and robustness of the proposed method. Although the processing time is slightly longer than the time of other methods, the overall consumption time is relatively short due to images acquired by a convenient device, which illustrates the high efficiency of the proposed method. Meanwhile, we developed two new models based on the pre-trained VGG-16 net [37] and our proposed MSnet to directly predict fabric density. The architectures of the two models are shown in Table 7. Although we used Dropout [38] to avoid overfitting, directly predicting fabric density has low performance on the testing set. The reasons may be that the dataset has a little imbalance and the directly predicted models have some drawbacks.

VI. CONCLUSION

In this research, we propose a novel woven fabric measurement method based on yarns locating by using MSnet. The method can locate warps and wefts and accurately measure woven fabric density. Extensive experimental results demonstrate that: 1) the proposed method reaches high accuracy compared with other automatic methods, 2) the proposed method shows good robustness under various kinds of patterns and densities fabrics, and 3) the proposed method can measure fabric density efficiently and conveniently. Despite of the high performance of fabric density measurement, the proposed method has some limitation when dealing with curved yarns fabrics and nonuniform density fabrics. In the future, we will continue to further improve the performance of the proposed method and develop new end-to-end model to automatically measure fabric density and identify more other fabric parameters.

REFERENCES

- [1] D. Schneider, Y. S. Gloy, and D. Merhof, "Vision-Based On-Loom Measurement of Yarn Densities in Woven Fabrics," *IEEE Transactions on Instrumentation & Measurement*, vol. 64, pp. 1063-1074, 2015.
- [2] "Textiles—Woven fabrics—Construction—Methods of analysis—Part 2: Determination of number of threads per unit length," ed. ISO 7211-2: Switzerland: International Organization for Standardization(ISO), 1999.
- [3] B. Xu, "Identifying fabric structures with fast Fourier transform techniques," *Textile Research Journal*, vol. 66, pp. 496-506, 1996.
- [4] E. J. Wood, "Applying Fourier and associated transforms to pattern characterization in textiles," *Textile Research Journal*, vol. 60, pp. 212-220, 1990.
- [5] W. Gao, J. Liu, B. Xu, W. Di, and W. Xue, "Automatic identification of weft arrangement parameters in fabric," *Cotton Textile Technology*, vol. 30, pp. 28-31, 2002.
- [6] E. Aldemir, H. Özdemir, and Z. Sari, "An improved gray line profile method to inspect the warp-weft density of fabrics," *The Journal of The Textile Institute*, pp. 1-12, 2018.
- [7] J. Zhang, R. Pan, W. Gao, and D. Zhu, "Automatic inspection of yarn-dyed fabric density by mathematical statistics of sub-images," *The Journal of The Textile Institute*.
- [8] Y. J. Jeong and J. Jang, "Applying image analysis to automatic inspection of fabric density for woven fabrics," *Fibers & Polymers*, vol. 6, pp. 156-161, 2005.
- [9] J. Zhang, W. GAO, and R. PAN, "A backlighting method for accurate inspection of woven fabric density," *DE REDACTIE*, p. 31, 2017.
- [10] R. Zhang and B. Xin, "An investigation of density measurement method for yarn-dyed woven fabrics based on dual-side fusion technique," *Measurement Science & Technology*, vol. 27, p. 085403, 2016.
- [11] H. S. Kim, S. H. Park, J. H. Ha, T. Y. Song, S. Y. Cho, and Y. K. Kim, "Development of a beta gauge system for a fabric density measurement," *Applied Radiation and Isotopes*, vol. 67, pp. 1213-1215, 2009.
- [12] Z. Jie, P. Ruru, and G. Weidong, "Automatic inspection of density in yarn-dyed fabrics by utilizing fabric light transmittance and Fourier analysis," *Applied Optics*, vol. 54, pp. 966-72, 2015.

- [13] J. Jing, S. Liu, P. Li, Q. Li, S. Liu, and M. Jiang, "Automatic density detection of woven fabrics via wavelet transform," *JOURNAL OF INFORMATION & COMPUTATIONAL SCIENCE*, vol. 11, pp. 2559-2568, 2014.
- [14] Y. Qin and F. Xu, "Analysis and research of the fabric density based on the wavelet transform," in *2012 Fifth International Symposium on Computational Intelligence and Design*, 2012, pp. 197-200.
- [15] J.-J. Lin, "Applying a co-occurrence matrix to automatic inspection of weaving density for woven fabrics," *Textile research journal*, vol. 72, pp. 486-490, 2002.
- [16] X. Wang and X. Li, "Recognition of fabric density with quadratic local extremum," *International Journal of Clothing Science and Technology*, vol. 24, pp. 328-338, 2012.
- [17] R. Pan, W. Gao, J. Liu, and H. Wang, "Automatic inspection of woven fabric density of solid colour fabric density by the Hough transform," *Fibres & Textiles in Eastern Europe*, vol. 18, p. 81, 2010.
- [18] R. Pan, W. Gao, J. Liu, and H. Wang, "Automatic detection of the layout of color yarns for yarn-dyed fabric via a FCM algorithm," *Textile research journal*, vol. 80, pp. 1222-1231, 2010.
- [19] R. Pan, J. Zhang, Z. Li, W. Gao, B. Xu, and W. Li, "Applying image analysis for automatic density measurement of high-tightness woven fabrics," *Fibres & Textiles in Eastern Europe*, 2016.
- [20] O. Ronneberger, P. Fischer, and T. Brox, "U-Net: Convolutional Networks for Biomedical Image Segmentation," 2015.
- [21] C. Szegedy, W. Liu, Y. Jia, P. Sermanet, S. Reed, D. Anguelov, et al., "Going deeper with convolutions," in *Proceedings of the IEEE conference on computer vision and pattern recognition*, 2015, pp. 1-9.
- [22] A. Krizhevsky, I. Sutskever, and G. E. Hinton, "Imagenet classification with deep convolutional neural networks," in *Advances in neural information processing systems*, 2012, pp. 1097-1105.
- [23] Y. Zhang, D. Zhou, S. Chen, S. Gao, and Y. Ma, "Single-image crowd counting via multi-column convolutional neural network," in *Proceedings of the IEEE conference on computer vision and pattern recognition*, 2016, pp. 589-597.
- [24] X. Cao, Z. Wang, Y. Zhao, and F. Su, "Scale aggregation network for accurate and efficient crowd counting," in *Proceedings of the European Conference on Computer Vision (ECCV)*, 2018, pp. 734-750.
- [25] W. Xie, J. A. Noble, and A. Zisserman, "Microscopy cell counting and detection with fully convolutional regression networks," *Computer methods in biomechanics and biomedical engineering: Imaging & Visualization*, vol. 6, pp. 283-292, 2018.
- [26] G. French, M. Fisher, M. Mackiewicz, and C. Needle, "Convolutional neural networks for counting fish in fisheries surveillance video," *Proceedings of the Machine Vision of Animals and their Behaviour (MVAB)*, pp. 7.1-7.10, 2015.
- [27] D. Merget, M. Rock, and G. Rigoll, "Robust facial landmark detection via a fully-convolutional local-global context network," in *Proceedings of the IEEE conference on computer vision and pattern recognition*, 2018, pp. 781-790.
- [28] M. Kowalski, J. Naruniec, and T. Trzcinski, "Deep alignment network: A convolutional neural network for robust face alignment," in *Proceedings of the IEEE Conference on Computer Vision and Pattern Recognition Workshops*, 2017, pp. 88-97.
- [29] K. Zhang, Y. Yan, P. Li, J. Jing, X. Liu, and Z. Wang, "Fabric Defect Detection Using Saliency Metric for Color Dissimilarity and Positional Aggregation," *IEEE Access*, vol. 6, pp. 49170-49181, 2018.
- [30] J. Xiang, N. Zhang, R. Pan, and W. Gao, "Fabric Image Retrieval System Using Hierarchical Search Based on Deep Convolutional Neural Network," *IEEE Access*, 2019.
- [31] Z. Wang, A. C. Bovik, H. R. Sheikh, and E. P. Simoncelli, "Image quality assessment: from error visibility to structural similarity," *IEEE Trans Image Process*, vol. 13, pp. 600-12, Apr 2004.
- [32] R. O. Duda and P. E. Hart, "Use of the Hough Transform to Detect Lines and Curves in Pictures," *Cacm*, vol. 15, pp. 11-15, 1972.
- [33] N. Ohtsu, "A Threshold Selection Method from Gray-Level Histograms," *IEEE Transactions on Systems Man & Cybernetics*, vol. 9, pp. 62-66, 1979.
- [34] T. Y. Zhang and C. Y. Suen, "A fast parallel algorithm for thinning digital patterns," *Comm Acm*, vol. 27, pp. 236-239, 1984.
- [35] X. Glorot and Y. Bengio, "Understanding the difficulty of training deep feedforward neural networks," *Proceedings of the thirteenth international conference on artificial intelligence and statistics*, vol. 9, pp. 249-256, 2010.
- [36] D. P. Kingma and J. Ba., "Adam: A method for stochastic optimization," *arXiv preprint arXiv:1409.1556*, 2014.
- [37] K. Simonyan and A. Zisserman, "Very deep convolutional networks for large-scale image recognition," *arXiv preprint arXiv:1409.1556*, 2014.
- [38] N. Srivastava, G. Hinton, A. Krizhevsky, I. Sutskever, and R. Salakhutdinov, "Dropout: A Simple Way to Prevent Neural Networks from Overfitting," *Journal of Machine Learning Research*, vol. 15, pp. 1929-1958, 2014.